Chaos
An Interdisciplinary Journal
of Nonlinear Science

AIP Publishing

Theory and experiments of spiral unpinning in the Belousov-Zhabotinsky reaction using a circularly polarized electric field

S V Amrutha,[1] Anupama Sebastian,[1] Puthiyapurayil Sibeesh,[1] Shreyas Punacha,[1,2] and T K Shajahan[1]
[1)]*Department of Physics, National Institute of Technology Karnataka, Mangalore, India-575025*
[2)]*Department of Oral Health Sciences, School of Dentistry, University of Washington, Seattle, WA 98195, USA*

(*Electronic mail: shajahan@nitk.edu.in)

(Dated: 3 May 2023)

We present the first experimental study of unpinning an excitation wave using a circularly polarized electric field. The experiments are conducted using the excitable chemical medium, the Belousov Zhabotinsky (BZ) reaction, which is modeled with the Oregenator model. The excitation wave in the chemical medium is charged, so it can directly interact with the electric field. This is a unique feature of the chemical excitation wave. The mechanism of wave unpinning in the BZ reaction with a circularly polarized electric field is investigated by varying the pacing ratio, the initial phase of the wave, and field strength. The chemical wave in the BZ reaction unpins when the electric force opposite the direction of the spiral is equal to or above a threshold. We developed an analytical relation of the unpinning phase with the initial phase, the pacing ratio, and the field strength. This is then verified in experiments and simulations.

Excitable systems, such as the Belousov-Zhabotinsky(BZ) reaction, cardiac tissue, nerve cells, and aggregation of slime mold amoeba, exhibit spatio-temporal patterns that include expanding target waves and rotating spiral waves. Spiral waves in such systems are of special interest since, once formed, a spiral wave continues to rotate inside the medium. Rotating spiral waves underlie cardiac arrhythmias like ventricular tachycardia and fibrillation. Several studies have shown that such spiral waves can interact with heterogeneities in the tissue and get pinned to it, forming a stable rotating wave around the boundary of the heterogeneity. Such pinned waves are very difficult to remove from the medium, so unpinning has attracted many groups studying excitable waves. An external electric field can help unpinning, provided they are applied in a specific way. The efficacy of unpinning depends on the details of the interaction between the wave and the field. In a cardiac system, the field induces secondary wave emission from the heterogeneity, and the high-frequency secondary waves lead to unpinning. In this paper, we study unpinning of chemical waves using a circularly polarized electric field (CPEF). We do not observe any secondary waves in the chemical medium. Instead, the electric field exerts a force directly on the chemical wavefront. The chemical wave is unpinned when the electric force is opposite to the direction of the wave propagation. We measure the angle at which the chemical wave leaves the heterogeneity. We show that this angle depends on the initial angle of the wave, frequency, and strength of the rotating electric field.

I. INTRODUCTION

The Belousov-Zhabotinsky (BZ) reaction has served as the prototype of a large class of systems that display excitation waves, including the waves of action potentials seen in the heart[1,2], brain[3], retina[4], and waves of communication in the social amoeba Dictyostelium discoideum[5,6]. Excitation waves in these systems exhibit strikingly similar spatio-temporal patterns such as expanding target waves[7] or rotating spiral waves[8–11]. Recently there has been a renewed interest in the pattern formation in the BZ reaction because of the active nature of the chemical waves: their wavefronts are electrically charged[12,13], and it is shown that droplets of BZ reagents in an oily medium can self-propel[14–16].

A characteristic feature of rotating excitation waves is their tendency to pin to heterogeneities in the medium[17–20]. A pinned rotating wave requires a carefully administered stimulus to remove it from the heterogeneity[21]. This is especially pertinent in cardiac tissue since stable, rotating waves can be life-threatening[21,22]. Several groups have proposed methods for controlling such pinned waves using either pulsed electric field[1,23] or, more recently, circularly polarized electric field[24–26]. A polarized electric field can be generated by applying two alternating electric fields simultaneously along the X and Y axes. By varying the phase difference between the two fields, different types of polarized electric fields can be obtained. If the phase difference is $\pi/2$, the resulting field will rotate with a constant amplitude at a uniform rate. So, the resultant field vector traces out a circle; hence, it is known as a circularly polarized electric field (CPEF). Numerical studies have shown that circularly polarized electric fields (CPEF) are more efficient in controlling cardiac excitation waves[24,26,27]. In particular, CPEF requires less energy and is more efficient in controlling pinned rotating waves in models of cardiac tissue[24,25]. Our systematic investigations on the mechanism of CPEF in cardiac models indicated that the spiral wave could be unpinned if the frequency of the CPEF is more than a cut-off frequency[27].

It is observed that chemical waves are also prone to pinning[17], and they can also be unpinned using electric field[12,28,29]. However, there is an essential distinction between the chemical wave and the waves in physiological tissue. In the latter, the electric force does not affect the excitation wave directly; instead, they unpin by inducing secondary excitations from the heterogeneities[30]. In the chemical medium, on the other hand, the wavefront contains charged ions such as

Br^- and Fe^{3+}, which can be moved by the applied electric field, *i.e.*, the electric field in a chemical medium exerts an advective force directly on the wavefront[12,31,32]. The physiological tissue does not report such an electric force on the wave. It is also observed that the chemical wave unpins as the tip moves away from the anode, and not when moving towards it[12]. So far, there have not been any experimental reports of unpinning spiral waves using CPEF, either in the chemical medium or the cardiac tissue. This paper reports the first experimental studies of spiral wave unpinning using CPEF in an excitable medium. However, the mechanism of how CPEF acts on a chemical wave differs from that of the cardiac excitation wave. In particular, we find no lower cut-off frequency for CPEF to unpin a chemical wave. We studied the unpinning by varying the pacing ratio, initial spiral phase, and field strength. We observed that the wave unpins when the component of the electric field vector along the direction of the spiral equals or exceeds a critical field strength. Based on this, we predict the unpinning phase of the spiral as a function of the initial position of the spiral wave, the pacing ratio, and the strength of the electric field. A CPEF can provide a wide range of spiral unpinning phases depending on the value of the pacing ratio. Hence, for a particular field strength, the chance of unpinning is more with an applied CPEF. We show that our analytical formulation agrees with experimental data and numerical results.

II. METHODS

A. Experiment

This paper focuses on unpinning an anticlockwise (ACW) rotating spiral using a CPEF rotating in the same direction. We conducted our studies in the ferroin-catalyzed BZ reaction in a petri-dish[12]. We start with the following initial reagent concentrations: $[H_2SO_4]$ = 0.16 M, $[NaBrO_3]$ = 40 mM, $[CH_2(COOH)_2]$ = 40 mM, and $[Fe(phen)_3SO_4]$ = 0.5 mM. The stock solutions are prepared using deionized water. The reaction mixture is embedded in 0.8 % w/v of agar gel to avoid hydrodynamic perturbations. The reagents are added individually to the initially boiled and cooled mixture of agar and deionized water. The reaction mixture is poured into a glass petri-dish after one color oscillation. The single reaction layer of thickness 3 mm is taken in a glass petri dish of diameter 10 cm.

A circular excitation wave is created at the center of the reaction medium by touching the surface with a silver wire during gelation. By disrupting the motion of the circular wavefront, a pair of counter-rotating spirals are created. To generate a pinned spiral wave, a glass bead of diameter 1.2 mm is carefully placed at the tip of one of the spirals. By inserting only half of the bead into the gel (Fig. 1(a)), we ensure the spiral pin to the great circle of the spherical bead. The pinning of the spiral tip to the obstacle is confirmed after 1-2 rotations. Our experiments are conducted in thin gel with a thickness smaller than the wavelength of spiral propagation ($\lambda = 3.7$ mm). The chemical wave does not develop a three-dimensional structure when the thickness is smaller than the wavelength. An anticlockwise rotating circularly polarized electric field (CPEF) is applied using two pairs of copper electrodes as in Fig. 1(a). The electrodes are fixed in the medium using electrode holders (Check the supplementary material to see the electrode arrangement). Images of the reaction medium are recorded using a CCD camera at every 0.5 s interval for $1-2$ hours.

B. Simulation

To model this experiment, we use a two-dimensional Oregonator model. The model equations are given by

$$\frac{\partial u}{\partial t} = \frac{1}{\varepsilon}(u(1-u) - \frac{fv(u-q)}{u+q}) + D_u\nabla^2 u + M_u(\vec{E}\cdot\nabla u) \quad (1)$$

$$\frac{\partial v}{\partial t} = u - v + D_v\nabla^2 v + M_v(\vec{E}\cdot\nabla v). \quad (2)$$

Here, u is the activator variable, and v is the inhibitor variable (corresponding to the rescaled concentrations of $HBrO_2$ and the catalyst $Fe(phen)_3SO_4$, respectively). The values of the diffusion coefficients are D_u = 1.0 and D_v = 0.6. Here, M_u and M_v describe the ionic mobilities of the activator and inhibitor variable respectively. We have taken M_u = 1.0 and M_v = -2.0 in our simulations. $\vec{E} = E_0 cos(\frac{2\pi t}{T})\hat{x} + E_0 sin(\frac{2\pi t}{T})\hat{y}$ is the circularly polarized electric field. The electric field is added as an advection term for the variables u and v.

The activator, u, triggers the reaction and diffusion processes. By lowering the diffusion coefficient, D_u, the cell-to-cell coupling can be reduced[33]. So, lowering the values of u and D_u close to zero results in a non-excitable obstacle. The circular obstacle of radius $r = 1.0$ s.u is created at the domain center by setting $u = 0$ at $t = 0$ t.u and lowering D_u to 0.0001. We implement non-flux boundary conditions on both the obstacle as well as the domain boundary using the phase field method[34]. Details of the model and the simulations are given in Ref.[12].

III. RESULTS AND DISCUSSIONS

The rotating chemical wave in the BZ reaction medium can get anchored into the boundary of the glass bead and form a very stable pinned wave, as shown in Fig. 1(b). A similar situation occurs in the numerical simulation of the model equations, where the spiral wave can get anchored to the obstacle in the domain. Here, we use a circularly polarized electric field (CPEF) to unpin the anchored spiral tip from the obstacle. In experiments, we employ a CPEF using two cross-electrodes (see Fig 1.(a)).

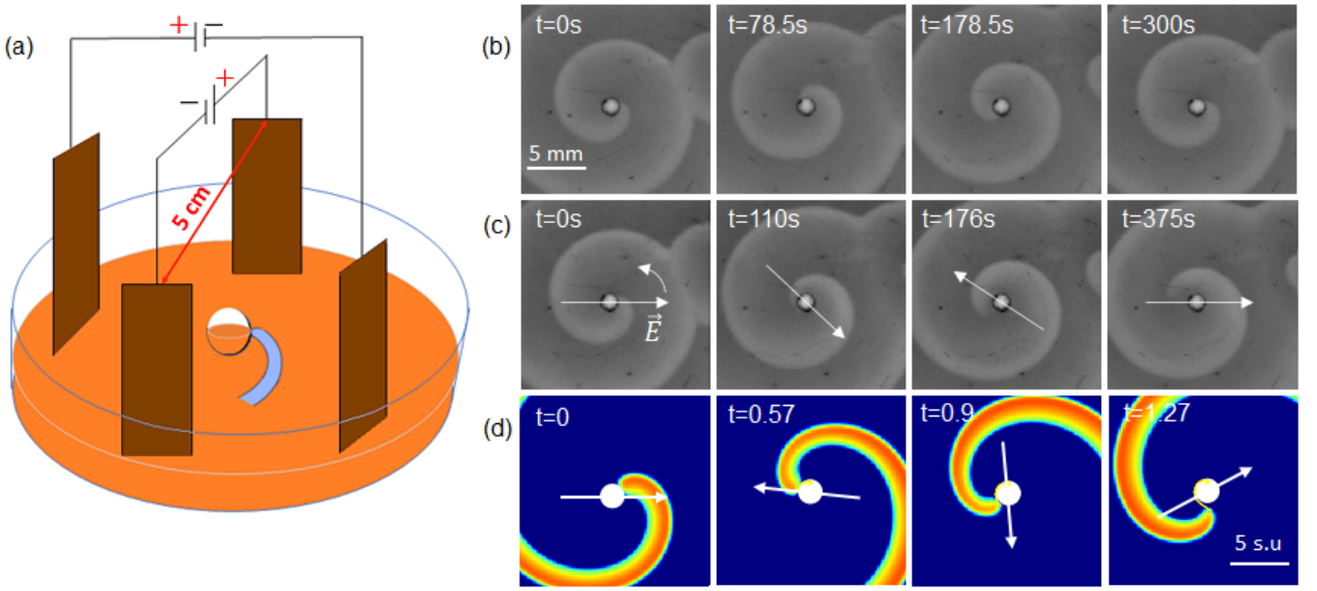

FIG. 1. **(a) Schematic diagram of the experimental system:** The positions of two pairs of field electrodes with respect to the glass bead are shown schematically (not to scale). **Unpinning of an anti-clockwise rotating spiral using CPEF:** (b) An ACW rotating spiral pinned to a spherical bead of diameter 1.2 mm in the experiment. The natural period of pinned spiral tip $T_s = 297$ s. (c) An applied CPEF of strength $E_0 \simeq 1.38$ V/cm, and period $T_E = 125$ s unpins the spiral tip from the obstacle. (d) An ACW rotating spiral pinned to an obstacle of diameter 1.0 s.u in the simulation with $T_s = 1.77$ t.u is subjected to a CPEF of strength $E_0 \simeq 0.6$ and period $T_E = 1.18$ t.u. The unpinned spiral tip drifts away from the obstacle at t = 1.27 t.u. The arrows show the direction of the applied CPEF. Area of each captured frame is 1.5 cm $\times$ 1.5 cm. (See the video in the supplementary material)

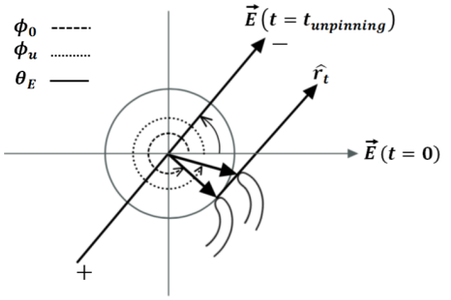

FIG. 2. Schematic diagram showing the phase measurements: ϕ_0 and ϕ_u are the phase of the spiral tip at $t = 0$ and at the time of unpinning respectively. θ_E denotes the phase of the electric field $\vec{E}$ and $\hat{r}_t$ is the tangential vector of spiral rotation on the obstacle boundary. All phases are measured in the anticlockwise direction from the $+x$ axis, with the obstacle center as the origin. The tail of the resultant field vector $\vec{E}$ marked with a $+$ sign is mentioned as the anode and the head with a $-$ sign is the cathode.

The CPEF can unpin the wave if the amplitude of the resultant electric field (E_0) equals or exceeds a certain threshold value (E_{th}), as shown in Fig. 1(c). The arrow in the figure indicates the instantaneous direction of the electric field. Similar unpinning is also seen in the simulations [Fig. 1(d)]. To understand the unpinning process, we measure the location at which the wave unpins from the obstacle. We can quantify the spiral location by the phase of the spiral tip on the obstacle boundary. The phase is the angle of the spiral tip, measured in degrees from the $+x$-axis along the anticlockwise direction with the obstacle center as the origin. The phase of the spiral when we start the CPEF is denoted by ϕ_0 and the phase when the spiral unpins from the boundary is denoted by ϕ_u [Fig. 2]. The instantaneous direction of the electric field is denoted by the angle θ_E. The direction of the spiral propagation is along the tangent at the obstacle boundary, and this direction is denoted by $\hat{r}_t$. We define the pacing ratio, p, as the ratio of the frequency of the CPEF (ω_{cp}) to that of the spiral (ω_s), *i.e.*, $p = \omega_{cp}/\omega_s$. We have varied p from 0.25 to 3.

Our observations can be summarised as follows: (1) The chemical wave can be unpinned with CPEF for all pacing ratios (between 0.25 to 3), provided the strength of the electric field (E_0) is equal or above a threshold. There is no lower cut-off frequency, and both overdrive pacing ($p > 1$) and underdrive pacing ($p < 1$) are equally effective. (2) The spiral unpinning phase ϕ_u varies linearly with ϕ_0. It increases for overdrive pacing and decreases for underdrive pacing (Fig. 3). (3) (ϕ_u- ϕ_0) varies with the pacing ratio, p, as in Fig. 4. (4) Unpinning is not guaranteed within one rotation of the spiral. *i.e.*, in comparison with a DC field[12], the time taken for unpinning with a CPEF can be more than a rotational period of the spiral tip. (5) In a few cases, where either the relative rotation of the spiral-field pair varies quickly (extremely overdrive or underdrive pacing), or ϕ_0 lies close to the expected ϕ_u (*i.e.*, (ϕ_u - ϕ_0) ≈ 0), the spiral misses unpinning at the first expected phase. Here, the unpinning may happen later at a phase where the unpinning condition is satisfied again (dashed lines in Fig. 4). (6) It takes several rotations for the chemical wave

to unpin as p approaches 1 (when the spiral and the CPEF rotate with the same frequency). The wave cannot be unpinned for resonant pacing ($p = 1$) except for a small range of initial conditions (ϕ_0). This range increases with the strength of the electric field (Fig. 5).

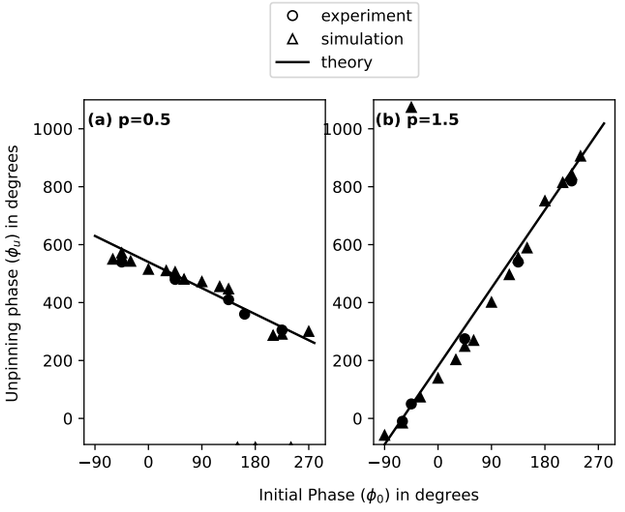

FIG. 3. **Unpinning at $E_0 = E_{th}$:** (a) The unpinning phase ϕ_u is plotted against ϕ_0 for p = 0.5 (underdrive pacing). (b) same as (a) but for p = 1.5 (overdrive pacing). In both cases ϕ_u varies linearly with ϕ_0. Circles and triangles represent the experiment and simulation data respectively.

These results can be analyzed in light of our recent work with the DC electric fields[12]. We found that the electric field exerts a retarding force on the chemical wavefront, which is maximum when the field direction is along the direction of the wavefront. For a CPEF with field strength $E_0 = E_{th}$ this condition is satisfied when $\vec{E} \cdot \hat{r}_t = E_{th}$. Here, $\hat{r}_t = -sin\phi_s\hat{x} + cos\phi_s\hat{y}$, where ϕ_s is the spiral phase. From the above condition, we can estimate the unpinning spiral phase by solving the scalar product as,

$$\phi_u = \frac{p\phi_0 + 90^0}{p-1}; p > 1 \tag{3}$$

$$\phi_u = \frac{270^0 - p\phi_0}{1-p}; p < 1 \tag{4}$$

When $E_0 = E_{th}$, the wave unpins only when $\theta_E - \phi_0 = 90^0$. The theoretical solid curves in Figs. 3 and 4 are based on the above equation.

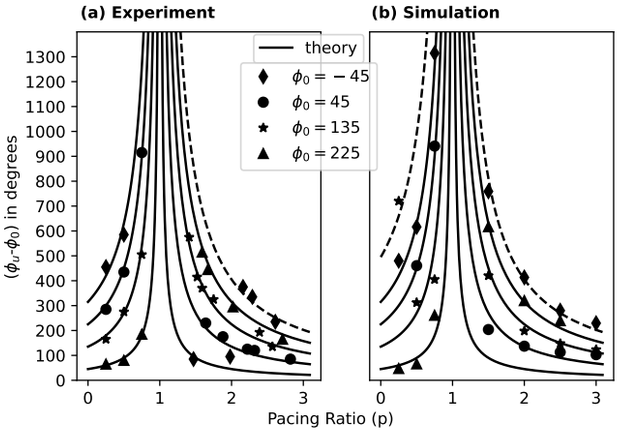

FIG. 4. **Unpinning at $E_0 = E_{th}$:** For spirals with different ϕ_0, the phase difference (ϕ_u- ϕ_0) is plotted (solid curve) with the pacing ratio, p in (a) experiments and (b) simulations. The solid theory lines represent the phases where the unpinning condition is satisfied for the first time (Eq.A9). The dashed lines at the top correspond to the phases where the spiral unpins when the unpinning condition is met a second time in its subsequent rotations. Most of the cases with $\phi_0 = -45^0$ show a delayed unpinning.

For a field strength greater than E_{th}, the wave must unpin when the component of $\vec{E}$ along $\hat{r}_t$ reaches the critical threshold, *i.e.*, $\vec{E} \cdot \hat{r}_t \geq E_{th}$. Solving and rearranging this condition gives an upper-bound and lower-bound for possible spiral unpinning phases ϕ_u. For overdrive pacing with $p > 1$, the unpinning phase window is given by

$$\frac{p\phi_0 + \sin^{-1}(\frac{E_{th}}{E_0})}{p-1} \leq \phi_u \leq \frac{p\phi_0 - \sin^{-1}(\frac{E_{th}}{E_0}) + \pi}{p-1} \tag{5}$$

with a width $\Delta\phi_u = \frac{\pi - 2\sin^{-1}(\frac{E_{th}}{E_0})}{p-1}$. In most cases, the unpinning condition (Eq. A6) is satisfied at the lower bound of this range. However, unpinning is possible at any point inside the window (refer to Appendix A).

For underdrive pacing *i.e.*, for $p < 1$, the unpinning phase window is

$$\frac{\pi + \sin^{-1}(\frac{E_{th}}{E_0}) - p\phi_0}{1-p} \leq \phi_u \leq \frac{2\pi - \sin^{-1}(\frac{E_{th}}{E_0}) - p\phi_0}{1-p} \tag{6}$$

The width of this window is $\Delta\phi_u = \frac{\pi - 2\sin^{-1}(\frac{E_{th}}{E_0})}{1-p}$. Depending on the strength of the electric field, the width of the window increases. The window reduces to a point when $E_0 = E_{th}$.

For p = 1, unpinning happens only if the following condition is satisfied.

$$\pi + \sin^{-1}(\frac{E_{th}}{E_0}) \leq \phi_0 \leq 2\pi - \sin^{-1}(\frac{E_{th}}{E_0}) \tag{7}$$

Thus for $p = 1$, the range of initial phases that lead to unpinning increases with the field strength, E_0. Figure. 5 shows the initial spiral phases that lead to successful unpinning as a function of $\frac{E_{th}}{E_0}$.

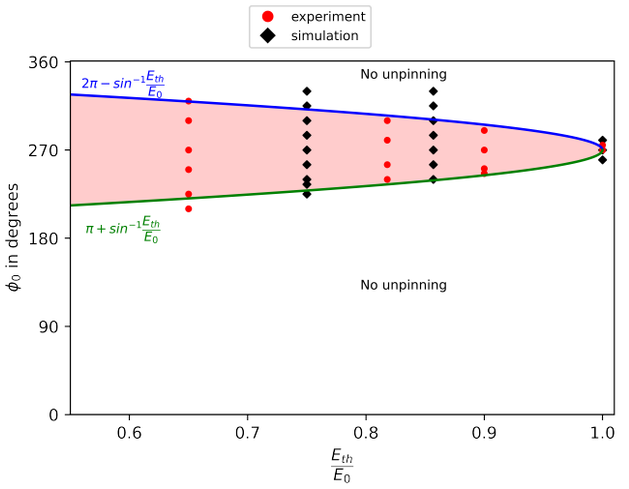

FIG. 5. Unpinning of spiral wave with pacing ratio, $p = 1$ for different field strength: $\pi + \sin^{-1}(\frac{E_{th}}{E_0})$ and $2\pi - \sin^{-1}(\frac{E_{th}}{E_0})$ are the lower and upper limit of the range of possible ϕ_0-values which gives successful unpinning for $p = 1$. The shaded region corresponds to the cases of successful unpinning. Circles and diamonds represent the experiment and simulation data respectively.

IV. CONCLUSIONS

In summary, we have presented the first experimental studies using a co-rotating circularly polarized electric field to unpin an excitation wave. In our studies, we have assumed that the rotating chemical wave is essentially two-dimensional. We observed unpinning with overdrive, underdrive and resonant pacing. Because of the charge on the chemical wavefront, the mechanism of chemical wave unpinning differs from that in other excitable media. The wave unpins when the electric field component along the tangential direction of spiral propagation is equal to or more than the critical threshold; *i.e.*, when the electric force opposite to the instantaneous spiral propagation is above the threshold value. Based on this condition, we can predict the unpinning phase, and the same has been verified in simulations and experiments. The unpinning phase depends on the pacing ratio, initial spiral phase, and applied field strength. For a particular field strength, the width of the unpinning phase window can be increased by varying the pacing ratio. This helps in increasing the chances of unpinning compared to a constant DC electric field.

We have seen from the previous studies that there is a fundamental difference in the mechanism of field-induced unpinning in biological and chemical excitable systems. Studies on electric field and chemical wave interactions in the BZ reaction have shown that the speed of the chemical wave increases as it propagates towards the anode, and it decreases as the wave moves away from the anode[32,35,36]. Moreover, wave splitting, annihilation, and extinction have also been observed in an external electric field. A free spiral wave in the BZ medium drifts with a parallel component which is always directed towards the anode, and a chirality-dependent perpendicular component[37]. The spiral drift is studied in numerous experimental and computational studies with DC, AC, and polarized electric fields[37–40]. The experimental observations were satisfactorily explained using the diffusion of ionic species in response to the applied electric field.

In the unpinning reported here, the wave always gets unpinned when the electric force is opposite to the wave propagation direction. The spiral never unpins while accelerating in the direction of electric force or while propagating toward the positive field polarity. The spiral wavefront behaves like a negatively charged particle in an external electric field. When the spiral propagates away from the positive field polarity, it experiences an electric force opposite to its propagation, and the tip unpins from the obstacle.

Our work reiterates the active nature of chemical waves- they are electrically charged and can directly interact with external electric fields. Recently people have started looking at interesting active properties of the BZ reaction. For example, it is shown that the chemical waves can induce changes in the surface tension profile on the droplets of BZ reaction, and it can lead to the self-propulsion of those droplets in oily media[14,16]. Our work indicates another way such active interactions can take place. We hope this will stimulate further studies into the dynamics of chemical waves and droplets.

V. SUPPLEMENTARY MATERIAL

A video (mp4) of spiral unpinning in the BZ experiments with an ACW rotating CPEF and an image of electrode arrangement are available as the supplementary material.

ACKNOWLEDGMENTS

We thank Beneesh P B, Deepu Vijayasenan, Ajith K M, V. Sreenath, K V Gangadharan, and Muhammed Mansoor C B for the discussions. Experiments were conducted using a grant (ECR/2016/000983) from Science and Engineering Research Board, Department of Science and Technology (SERB-DST), India.

AUTHOR CONTRIBUTIONS

S.V.A and T.K.S conceived the study. S.V.A performed the experiments, and P.S. built the experimental setup. S.P and A.S performed numerical simulations. S.V.A, A.S, and T.K.S analysed the data. A.S and T.K.S developed the theory. S.V.A and T.K.S wrote the paper. All authors helped to edit the paper.

Appendix A: Derivation of analytical formulae to calculate ϕ_u

$$\text{Electric field}, \vec{E} = E(cos\theta_E \hat{i} + sin\theta_E \hat{j}) \qquad \text{(A1)}$$

The spiral tangent vector, $\hat{r_t} = -sin\phi_s\hat{i} + cos\phi_s\hat{j}$ (A2)

The condition for unpinning is $\vec{E} \cdot r_t \geq E_{th}$. (A3)

$i.e., Esin(\theta_E - \phi_s) \geq E_{th}$ or $Esin(\pi - \theta_E + \phi_s) \geq E_{th}$ (A4)

At unpinning, $\phi_s = \phi_u$ and $\theta_E = p(\phi_u - \phi_0)$. (A5)

Plugging Eqn. A5 into Eqn.A4 will give,

$$\frac{p\phi_0 + \sin^{-1}(\frac{E_{th}}{E_0})}{p-1} \leq \phi_u \leq \frac{p\phi_0 - \sin^{-1}(\frac{E_{th}}{E_0}) + \pi}{p-1} \quad \text{(A6)}$$

Eqn. A6 on rearrangement and mapping to the positive angular coordinates by adding 2π, will give

$$\frac{\pi + \sin^{-1}(\frac{E_{th}}{E_0}) - p\phi_0}{1-p} \leq \phi_u \leq \frac{2\pi - \sin^{-1}(\frac{E_{th}}{E_0}) - p\phi_0}{1-p} \quad \text{(A7)}$$

At $E = E_{th}$, Eqn. A6 and Eqn. A7 will reduce to the following equations:

$$\phi_u = \frac{p\phi_0 + 90^0}{p-1}; p > 1 \quad \text{(A8)}$$

$$\phi_u = \frac{270^0 - p\phi_0}{1-p}; p < 1 \quad \text{(A9)}$$

At resonance pacing $p = 1$, The numerator of Eqn.A6 and Eqn.A7 should be set zero in order to get a definite value, which results in the condition

$$\pi + \sin^{-1}(\frac{E_{th}}{E_0}) \leq \phi_0 \leq 2\pi - \sin^{-1}(\frac{E_{th}}{E_0}) \quad \text{(A10)}$$

Appendix B: Unpinning for $E > E_{th}$

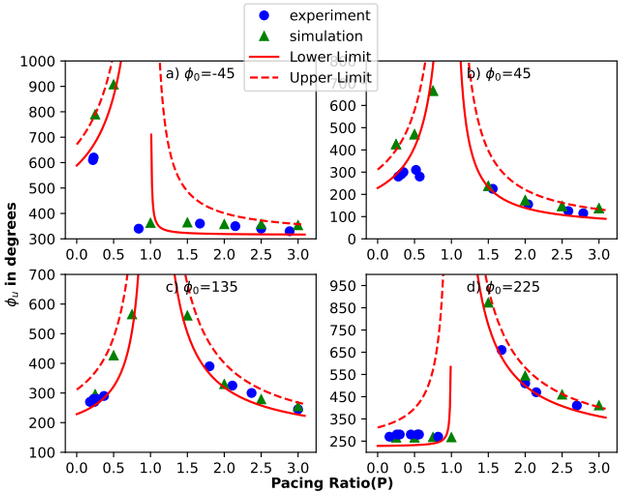

FIG. 6. Unpinning at $E > E_{th}$ ($\sin^{-1}(\frac{E_{th}}{E}) = 48.95^0$): Spiral waves with different ϕ_0 are unpinned in a CPEF with both under-drive ($p < 1$) and over-drive pacing ($p > 1$). The solid bottom line represents the lower limit of the range of possible ϕ_u-values given by the relation $\phi_u = (p\phi_0 + 48.95)/(p-1)$ for over-drive pacing and $\phi_u = (\pi - p\phi_0 + 48.95)/(1-p)$ for under-drive pacing. The upper limit of the range of possible ϕ_u-values, given by the relation $\phi_u = (p\phi_0 + \pi - 48.95)/(p-1)$ for over-drive pacing and $\phi_u = (2\pi - p\phi_0 - 48.95)/(1-p)$ for under-drive pacing, are represented by the top dashed line. Circles and triangles represent the experiment and simulation data, respectively.

Fig.6 shows the unpinning phase window at $E > E_{th}$ for different initial phases of the spiral. Here, the solid lines correspond to the lower limit, and the dashed lines correspond to the upper limit of the window according to equations 5 and 6 in the main text. The unpinning always happens at a phase within this range. The width of the window varies with the field strength.

Appendix C: Comparison between unpinning of spirals pinned to obstacles of different geometry

The results of spiral unpinning from spherical beads are presented in the paper. For comparison, we have performed similar experiments using cylindrical rods. The experimental setup is the same as in Fig.1a in the main text. A cylindrical glass rod of length ≈ 4 mm is inserted vertically into the medium.

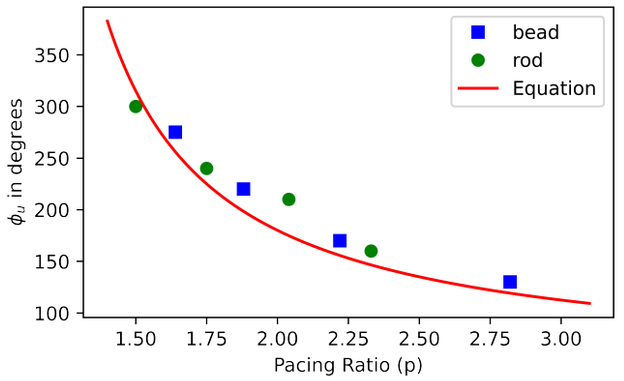

FIG. 7. Comparison of unpinning of spiral pinned to spherical bead and cylindrical rod: ϕ_u is plotted against the pacing ratio,p where $p > 1$. $\phi_0 = 45^0$ and E = 1.38 V/cm. The diameter of the obstacles are same and equals 1.2 mm.

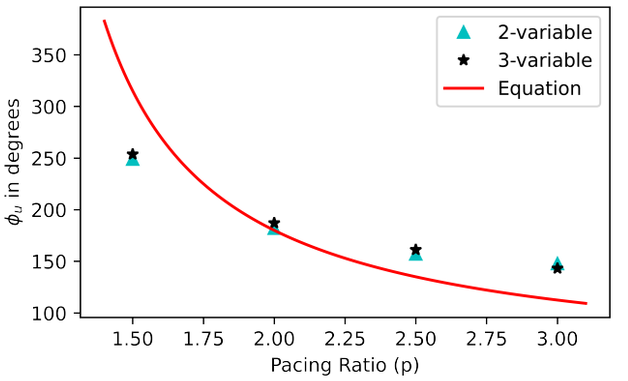

FIG. 8. Comparison of spiral unpinning obtained in two and three-variable Oregonator models: ϕ_u is plotted against the pacing ratio,p where $p > 1$. $\phi_0 = 45^0$ and E = 0.6. The obstacle diameter is 1.0 s.u.

Figure.7 shows the variation of unpinning phase with the pacing ratio for a cylindrical obstacle of radius 1.2 mm. The unpinning phases for a spherical bead have also been shown, and in both cases, unpinning occur at phases that are consistent with the theoretical predictions.

Appendix D: Comparison between numerical models

In this letter, we have used a two-variable reduction of the original three-variable Oregonator model. Here we compare the unpinning studies using both two and three-variable models.

The three-variable Oregonator model consists of the following equations[37].

$$\frac{\partial u}{\partial t} = \frac{1}{\varepsilon}(qw - uw + u(1-u)) + D_u\nabla^2 u \qquad \text{(D1)}$$

$$\frac{\partial v}{\partial t} = u - v + D_v\nabla^2 v + M_v(\vec{E}\cdot\nabla v) \qquad \text{(D2)}$$

$$\frac{\partial w}{\partial t} = \frac{1}{\varepsilon'}(-qw - uw + fv) + D_w\nabla^2 w + M_w(\vec{E}\cdot\nabla w) \qquad \text{(D3)}$$

The variables u, v and w represent the re-scaled dimensionless concentrations of $HBrO_2$, Fe^{3+}, and Br^- respectively. The model parameters are $q = 0.002$, $f = 1.4$, $\varepsilon = 0.01$ as in Numerical methods in the manuscript, along with an additional parameter, $\varepsilon' = 0.0001$. For both variables v and w, the electric field $\vec{E}$ is added as an advection term. However, the variable u is unaffected in an electric field as it corresponds to the charge-less species $HBrO_2$. The values of the ionic mobilities are M_u = 0, M_v = -2, and M_v = 1. Our recent paper[12] shows the simulation details.

Using the three-variable model, we measured the unpinning phase of an ACW spiral pinned to an obstacle of radius, r=1.0 s.u in an electric field of strength E_{th} = 0.6. The unpinning is done for a fixed initial phase with overdrive pacing. The results are in good agreement with those obtained from the two-variable Oregonator model and the theory (Figure.8).

[1] S. Luther, F. H. Fenton, B. G. Kornreich, A. Squires, P. Bittihn, D. Hornung, M. Zabel, J. Flanders, A. Gladuli, L. Campoy, and *et al.*, "Low-energy control of electrical turbulence in the heart," Nature **475**, 235–9 (2011).
[2] K. Diagne, T. M. Bury, M. W. Deyell, Z. Laksman, A. Shrier, G. Bub, and L. Glass, "Rhythms from two competing periodic sources embedded in an excitable medium," Phys. Rev. Lett. **130**, 028401 (2023).
[3] X. Huang, W. C. Troy, Q. Yang, H. Ma, C. R. Laing, S. J. Schiff, and J.-Y. Wu, "Spiral waves in disinhibited mammalian neocortex." J. Neurosci. **24**, 9897–902 (2004).
[4] Y. Yu, L. M. Santos, L. A. Mattiace, M. L. Costa, L. i. C. Ferreira, K. Benabou, A. H. Kim, J. Abrahams, M. V. Bennett, and R. Rozental, "Reentrant spiral waves of spreading depression cause macular degeneration in hypoglycemic chicken retina," Proc. Natl. Acad. Sci. U.S.A. **109**, 2585–2589 (2012).
[5] J. Noorbakhsh, D. J. Schwab, A. E. Sgro, T. Gregor, and P. Mehta, "Modeling oscillations and spiral waves in dictyostelium populations," Phys. Rev. E **91**, 062711 (2015).
[6] K. Kamino, Y. Kondo, A. Nakajima, M. Honda-Kitahara, K. Kaneko, and S. Sawai, "Fold-change detection and scale invariance of cell–cell signaling in social amoeba," Proc. Natl. Acad. Sci. U.S.A. **114**, E4149–E4157 (2017).
[7] A. Zaikin and A. Zhabotinsky, "Concentration wave propagation in two-dimensional liquid-phase self-oscillating system," Nature **225**, 535–537 (1970).
[8] Y. Zhang, F. Wu, C. Wang, and J. Ma, "Stability of target waves in excitable media under electromagnetic induction and radiation," Phys. A: Stat. Mech. Appl. **521**, 519–530 (2019).
[9] V. S. Zykov, "Spiral wave initiation in excitable media," Philos. Trans. Royal Soc. A **376**, 20170379 (2018).
[10] S. Sinha and S. Sridhar, *Patterns in excitable media: Genesis, dynamics, and control* (CRC Press, 2014).
[11] A. T. Winfree, "Spiral waves of chemical activity," Science **175**, 634–636 (1972).
[12] S. V. Amrutha, A. Sebastian, P. Sibeesh, S. Punacha, and T. K. Shajahan, "Mechanism of spiral wave unpinning in the Belousov–Zhabotinsky reaction with a DC electric field," J. Phys. Chem. C **126**, 19618–19626 (2022).
[13] O. Steinbock, J. Schütze, and S. Müller, "Electric-field-induced drift and deformation of spiral waves in an excitable medium," Phys. Rev. Lett. **68**, 248 (1992).
[14] C. Jin, C. Krüger, and C. C. Maass, "Chemotaxis and autochemotaxis

of self-propelling droplet swimmers," Proc. Natl. Acad. Sci. U.S.A. **114**, 5089–5094 (2017).
[15]A. Ryabchun, D. Babu, J. Movilli, R. Plamont, M. C. Stuart, and N. Katsonis, "Run-and-halt motility of droplets in response to light," Chem **8**, 2290–2300 (2022).
[16]O. Back, M. Asally, Z. Wang, and Y. Hayashi, "Electrotaxis behavior of droplets composed of aqueous belousov-zhabotinsky solutions suspended in oil phase," Sci. Rep. **13**, 1340 (2023).
[17]M. Sutthiopad, J. Luengviriya, P. Porjai, M. Phantu, J. Kanchanawarin, S. C. Müller, and C. Luengviriya, "Propagation of spiral waves pinned to circular and rectangular obstacles," Phys. Rev. E **91**, 052912 (2015).
[18]Z. Y. Lim, B. Maskara, F. Aguel, R. Emokpae Jr, and L. Tung, "Spiral wave attachment to millimeter-sized obstacles," Circulation **114**, 2113–2121 (2006).
[19]C. W. Zemlin and A. M. Pertsov, "Anchoring of drifting spiral and scroll waves to impermeable inclusions in excitable media," Phys. Rev. Lett. **109**, 038303 (2012).
[20]T. K. Shajahan, S. Sinha, and R. Pandit, "Spiral-wave dynamics depends sensitively on inhomogeneities in mathematical models of ventricular tissue," Phys. Rev. E **75**, 11929 (2007).
[21]P. Bittihn, A. Squires, G. Luther, E. Bodenschatz, V. I. Krinsky, U. Parlitz, and S. Luther, "Phase-resolved analysis of the susceptibility of pinned spiral waves to far-field pacing in a two-dimensional model of excitable media," Philos. Trans. A. Math. Phys. Eng. Sci. **368**, 2221–36 (2010).
[22]R. Gray and J. Wikswo, "Cardiovascular disease: several small shocks beat one big one." Nature **475**, 181–2 (2011).
[23]S. Punacha, S. Berg, A. Sebastian, V. I. Krinski, S. Luther, and T. Shajahan, "Spiral wave unpinning facilitated by wave emitting sites in cardiac monolayers," Proc. R. Soc. A **475**, 20190420 (2019).
[24]X. Feng, X. Gao, D.-B. Pan, B.-W. Li, and H. Zhang, "Unpinning of rotating spiral waves in cardiac tissues by circularly polarized electric fields." Sci. Rep. **4**, 4831 (2014).
[25]D.-B. Pan, X. Gao, X. Feng, J.-T. Pan, and H. Zhang, "Removal of pinned scroll waves in cardiac tissues by electric fields in a generic model of three-dimensional excitable media," Sci. Rep. **6**, 1–8 (2016).
[26]X. Feng, X. Yin, J. Wen, H. Wu, and X. Gao, "Removal of spiral turbulence by virtual electrodes through the use of a circularly polarized electric field," Chaos **32**, 093145 (2022).
[27]S. Punacha, A. N K, and T. K. Shajahan, "Theory of unpinning of spiral waves using circularly polarized electric fields in mathematical models of excitable media," Phys. Rev. E **102**, 032411 (2020).
[28]M. Sutthiopad, J. Luengviriya, P. Porjai, B. Tomapatanaget, S. C. Müller, and C. Luengviriya, "Unpinning of spiral waves by electrical forcing in excitable chemical media," Phys. Rev. E **89**, 052902 (2014).
[29]A. Sebastian, S. Amrutha, S. Punacha, and T. Shajahan, "Dynamics of chemical excitation waves subjected to subthreshold electric field in a mathematical model of the belousov-zhabotinsky reaction," in *Nonlinear Dyn. and Appl.* (Springer, 2022) pp. 1241–1249.
[30]A. Pumir, V. Nikolski, M. Hörning, A. Isomura, K. Agladze, K. Yoshikawa, R. Gilmour, E. Bodenschatz, and V. Krinsky, "Wave emission from heterogeneities opens a way to controlling chaos in the heart," Phys. Rev. Lett. **99**, 208101 (2007).
[31]Z. A. Jiménez, Z. Zhang, and O. Steinbock, "Electric-field-controlled unpinning of scroll waves," Phys. Rev. E **88**, 052918 (2013).
[32]K. Agladze and P. De Kepper, "Influence of electric field on rotating spiral waves in the belousov-zhabotinskii reaction," J. Phys. Chem. **96**, 5239–5242 (1992).
[33]S. Alonso and A. V. Panfilov, "Negative filament tension in the luo-rudy model of cardiac tissue," Chaos: An Interdisciplinary Journal of Nonlinear Science **17**, 015102 (2007).
[34]F. H. Fenton, E. M. Cherry, A. Karma, and W.-J. Rappel, "Modeling wave propagation in realistic heart geometries using the phase-field method," Chaos: An Interdisciplinary Journal of Nonlinear Science **15**, 013502 (2005).
[35]R. Feeney, S. Schmidt, and P. Ortoleva, "Experiments on electric field- BZ chemical wave interactions: Annihilation and the crescent wave," Physica D: Nonlinear Phenomena **2**, 536–544 (1981).
[36]H. Ševčíková and M. Marek, "Chemical waves in electric field," Physica D: Nonlinear Phenomena **9**, 140–156 (1983).
[37]B. Schmidt and S. C. Müller, "Forced parallel drift of spiral waves in the belousov-zhabotinsky reaction," Phys. Rev. E **55**, 4390 (1997).
[38]V. Krinsky, E. Hamm, and V. Voignier, "Dense and sparse vortices in excitable media drift in opposite directions in electric field," Phys. Rev. Lett. **76**, 3854 (1996).
[39]J.-X. Chen, H. Zhang, and Y.-Q. Li, "Drift of spiral waves controlled by a polarized electric field," J. Chem. Phys. **124**, 014505 (2006).
[40]T.-C. Li, X. Gao, F.-F. Zheng, D.-B. Pan, B. Zheng, and H. Zhang, "A theory for spiral wave drift induced by ac and polarized electric fields in chemical excitable media," Sci. Rep. **7**, 1–9 (2017).